

## Experimental Test of Local Hidden-Variable Theories\*

Edward S. Fry and Randall C. Thompson

*Physics Department, Texas A & M University, College Station, Texas 77843*

(Received 10 June 1976)

We have measured the linear polarization correlation between the two photons from the  $7^3S_1 \rightarrow 6^3P_1 \rightarrow 6^1S_0$  cascade of  $\text{Hg}^{200}$ . The results were used to evaluate Freedman's version of the Bell inequality,  $\delta \leq 0$ . Our result is  $\delta_{\text{exp}} = +0.046 \pm 0.014$ , in clear violation of the inequality and in excellent agreement with the quantum mechanical prediction,  $\delta_{\text{QM}} = +0.044 \pm 0.007$ . An important feature of the experiment was the explicit measurement of the initial density matrix for the cascading atoms.

We have measured the linear polarization correlation of photon pairs from the  $7^3S_1 \rightarrow 6^3P_1 \rightarrow 6^1S_0$  cascade of  $\text{Hg}^{200}$ . Under appropriate experimental conditions, quantum mechanics (QM) predicts there should be a very strong correlation. The essence of Bell's theorem<sup>1</sup> is that any local hidden variable (LHV) theory restricts the strength of this correlation. This LHV restriction can be put in a form derived by Freedman,<sup>2</sup>

$$\delta = |R(67\frac{1}{2}^\circ)/R_0 - R(22\frac{1}{2}^\circ)/R_0| - \frac{1}{4} \leq 0. \quad (1)$$

Here the two photons are respectively detected on the  $\pm Z$  axes,  $R(\varphi)$  is the coincidence rate with an angle  $\varphi$  between the transmission axes of the polarizers, and  $R_0$  is the coincidence rate with polarizers removed. A decisive experimental test of LHV theories can then be obtained by choosing experimental conditions such that inequality (1) is violated by the quantum mechanical predictions.<sup>3</sup> Previously, results have been obtained from three such experiments. The first by Freedman and Clauser<sup>4</sup> used the calcium cascade  $6^1S_0 \rightarrow 4^1P_1 \rightarrow 4^1S_0$ . Their results violated the inequality and were in agreement with the QM predictions. The second by Holt<sup>5</sup> used the mercury ( $\text{Hg}^{198}$ ) cascade  $9^1P_1 \rightarrow 7^3S_1 \rightarrow 6^3P_0$ . The results satisfied the inequality and were in apparent disagreement with QM. The third, also by Clauser,<sup>6</sup> was recently completed using the same cascade in mercury ( $\text{Hg}^{202}$ ) and the same excitation technique as Holt. The results violated the inequality and were in agreement with QM.

The present experiment used a different cascade,  $7^3S_1 \rightarrow 6^3P_1 \rightarrow 6^1S_0$  in mercury ( $\text{Hg}^{200}$ ) (see Fig. 1). The  $7^3S_1$  state was populated in a two-step process, i.e., electron bombardment excitation to the  $6^3P_2$  state followed by absorption of resonant  $5461\text{-}\text{\AA}$  radiation from a laser. An atomic beam was used and the two excitation steps occurred at physically different locations. Consequently, in the interaction region (where the  $7^3S_1$

state is populated) there are essentially no rapidly decaying states other than the cascade states. Therefore there is a one-to-one correspondence between all  $4358\text{-}\text{\AA}$  and  $2537\text{-}\text{\AA}$  photons. As a result comparatively high data accumulation rates were obtained.

The experimental arrangement is shown in Fig. 2. The mercury atomic beam passes through a solenoid electron gun where atoms are excited to the  $6^3P_2$  state. Laser beams tuned to the resonant frequency of the  $5461\text{-}\text{\AA}$  transition in  $\text{Hg}^{200}$  intersect the atomic beam at two locations. The  $4358\text{-}\text{\AA}$  fluorescence from the first location provides a reference to lock the laser cavity onto the Hg resonance. The second location is the interaction region. Its dimensions, defined by the intersection of the two beams, are  $0.3 \times 0.8 \times 0.8 \text{ mm}^3$ . The first location is slightly off the atomic beam axis so that atoms which can "see" laser radiation in the first location cannot enter the interaction volume.

The laser radiation incident on the interaction region is polarized parallel to the  $Z$  axis. At the interaction region the emitted  $4358\text{-}\text{\AA}$  ( $2537\text{-}\text{\AA}$ ) photons are collected over a half-angle  $\theta = 19.9^\circ \pm 0.3^\circ$ , pass through a pile-of-plates polarizer and a filter, and are detected on the  $+(-) Z$  axis.

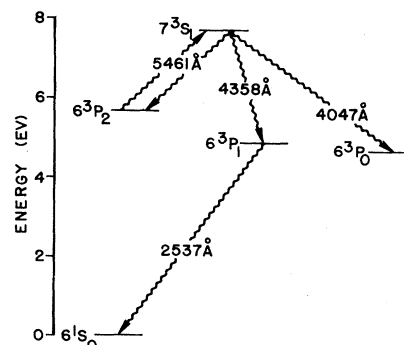


FIG. 1. Relevant energy levels and transitions in mercury.

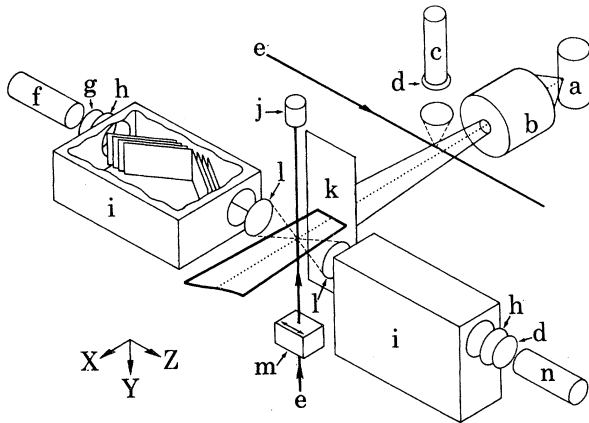


FIG. 2. Schematic of the apparatus. Polarizer plate arrangement is also indicated. Actual polarizers have 14 plates. (a) Hg oven; (b) solenoid electron gun; (c) RCA 8575; (d) 4358-Å filter; (e) 5461-Å laser beam; (f) Amperex 56 DUVF/03; (g) 2537-Å filter; (h) focusing lens; (i) pile-of-plates polarizer; (j) laser beam trap; (k) atomic beam defining slit; (l) light collecting lens; (m) crystal polarizer; (n) RCA 8850.

The collection optics are lens pairs whose radii have been adjusted to minimize the Seidel spherical aberration coefficient. Each polarizer consists of two sets of seven plates symmetrically arranged so as to cancel out transverse ray displacements. The magnetic field in the interaction region is zeroed to less than 5 mG in all directions.

A valid test can only be made with zero-spin isotopes. Our beam uses mercury of natural isotopic abundance; but we selectively excite only atoms of the zero-spin isotope, Hg<sup>200</sup>, to the initial state of the cascade by using 5461-Å radiation from a narrow-linewidth (15 MHz) tunable dye laser. By sweeping the laser frequency and observing the 4358-Å fluorescence we can ob-

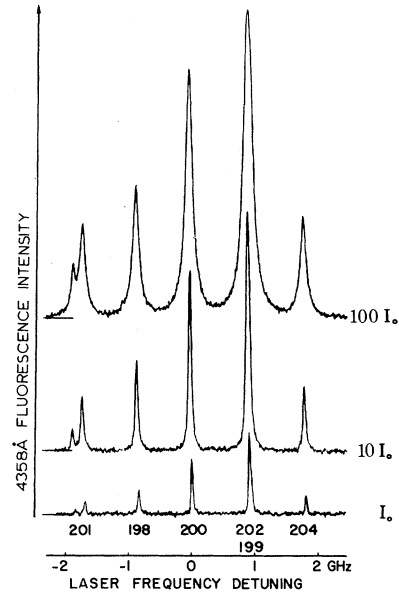


FIG. 3. Fluorescence intensity of 4358-Å radiation versus laser frequency for three intensities of the incident 5461-Å radiation. The lines for the various Hg isotopes are labeled with their mass numbers. The vertical scale is the same for all three scans; the zeroes have been offset for clarity.  $I_0 \sim 2.5 \text{ mW/cm}^2$ .

serve the structure of the 5461-Å absorption line.<sup>7</sup> Figure 3 shows the results for the central portion of the line for three incident laser intensities. The transition is power broadened, but at our operating intensity,  $I_0 \sim 2.5 \text{ mW/cm}^2$ , the isotope separation is very clean.

The initial state of our cascade has  $J=1$ . Its density matrix is  $3 \times 3$  and has elements  $\rho_{ij}$  where  $i$  and  $j$  are magnetic quantum numbers. With detectors on the  $\pm Z$  axes, the QM prediction for the coincidence rate  $S(\varphi)$  shows no dependence on  $\rho_{10}$  or  $\rho_{0-1}$ . (The coordinate system is indicated in Fig. 2.) When  $\rho_{1-1}$  is zero, the normalized coincidence rate is

$$R(\varphi)/R_0 = \frac{1}{4}(\epsilon_M^1 + \epsilon_m^1)(\epsilon_M^2 + \epsilon_m^2) - \frac{1}{4}(\epsilon_M^1 - \epsilon_m^1)(\epsilon_M^2 - \epsilon_m^2)F(\theta) \cos 2\varphi. \quad (2)$$

Here  $\epsilon_M^i$  ( $\epsilon_m^i$ ) is the transmission efficiency of the  $i$ th polarizer for light polarized parallel (perpendicular) to the transmission axis, and  $F(\theta)$  is given by

$$F(\theta) = \rho' J^2(\theta) [(1 + \rho')G^2(\theta) - (1 - 2\rho')G(\theta)H(\theta) - (2 - \rho')H^2(\theta)]^{-1}. \quad (3)$$

The functions<sup>8</sup>  $G(\theta)$ ,  $H(\theta)$ , and  $J(\theta)$  depend on the half-angle  $\theta$  subtended by the light collection optics, and  $\rho'$  is given by

$$\rho' = \rho_{00}/(\rho_{11} + \rho_{-1-1}). \quad (4)$$

It is essential to measure  $\rho'$ ; to check that  $\rho_{1-1}$  is zero; and to verify that the QM prediction, Eq.

(2), violates inequality (1).

The density matrix for atoms in the  $7^3S_1$  state is determined experimentally by measuring the polarization of the 4358-Å fluorescence at appropriate angles. It is found that at the high intensities at which the transition is saturated, the off-

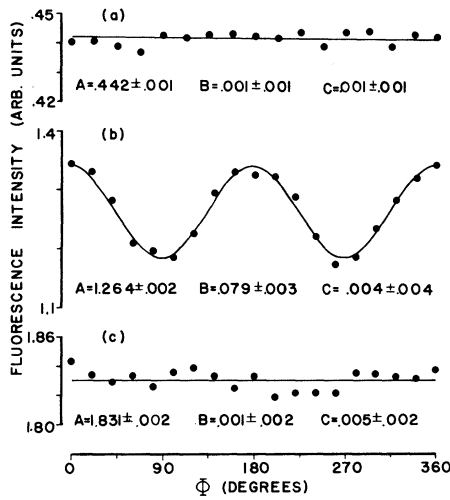


FIG. 4. Linear polarization dependences of the intensities of the cascade photons.  $\Phi$  is the angle of the polarizer transmission axis with respect to the  $X$  axis. The data are least-squares fitted by a function of the form  $A+B \cos 2\Phi+C \sin 2\Phi$  and the fitted parameters are given with each curve. (a) 4358- $\text{\AA}$  intensity on the  $+Z$  axis. (b) 4358- $\text{\AA}$  radiation detected on the  $-Y$  axis; from the fitted parameters we find  $\text{Re}(\rho_{10}-\rho_{0-1})=0$ , and  $\rho'=0.633 \pm 0.005$ . For completeness, Fig. 4(c) shows the polarization measurements of 2537- $\text{\AA}$  fluorescence on the  $-Z$  axis.

diagonal elements are nonzero and all elements are intensity dependent. With the intensity reduced to  $I_0 \sim 2.5 \text{ mW/cm}^2$ , our data (Fig. 4) show that the density matrix has the desired form. Figure 4(a) shows the results for the 4358- $\text{\AA}$  fluorescence on the  $+Z$  axis. The absence of a linear polarization dependence here implies  $\rho_{1-1}=0$ . Figure 4(b) shows the polarization measurements of 4358- $\text{\AA}$  radiation detected on the  $-Y$  axis; from the fitted parameters we find  $\text{Re}(\rho_{10}-\rho_{0-1})=0$ , and  $\rho'=0.633 \pm 0.005$ . For completeness, Fig. 4(c) shows the polarization measurements of 2537- $\text{\AA}$  fluorescence on the  $-Z$  axis.

The polarizer efficiency parameters are  $\epsilon_M^1=0.98 \pm 0.01$ ,  $\epsilon_M^2=0.97 \pm 0.01$ ,  $\epsilon_m^1=\epsilon_m^2=0.02 \pm 0.005$ . Hence the QM prediction, Eq. (2), for the normal-

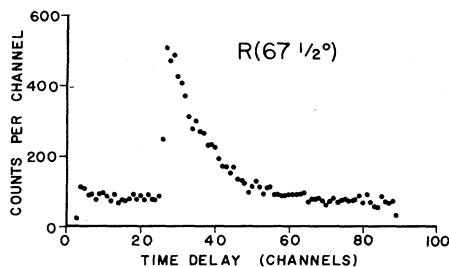


FIG. 5. Polarization coincidence spectrum. The total accumulation time is 80 min.

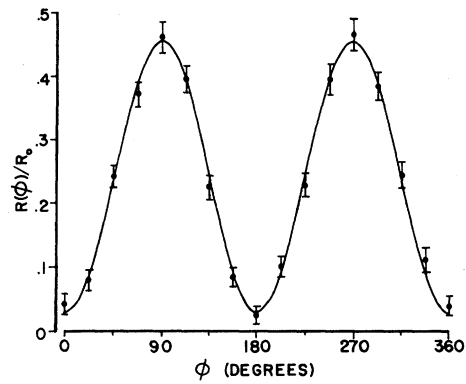


FIG. 6. Normalized polarization coincidence data from  $0^\circ$  to  $360^\circ$ . The datum point at  $0^\circ$  is duplicated at  $360^\circ$ . The smooth curve is a least-squares fit to  $R(\varphi)/R_0=A+B \cos 2\varphi+C \sin 2\varphi$ . The fitted parameters are  $A=0.242 \pm 0.003$ ;  $B=-0.212 \pm 0.004$ ;  $C=-0.003 \pm 0.004$ .

ized coincidence rate is

$$R(\varphi)/R_0 = (0.248 \pm 0.004) - (0.208 \pm 0.004) \cos 2\varphi \quad (5)$$

and we also find

$$\delta_{QM} = 0.044 \pm 0.007. \quad (6)$$

All errors are  $\pm 1$  standard deviation.

Coincidence data were obtained using a time-to-amplitude converter and a pulse-height analyzer. Figure 5 shows the total coincidence spectrum with  $67\frac{1}{2}^\circ$  between the polarizer axes. The total accumulation time for this spectrum was 80 min. To obtain the true coincidences, one must subtract out the accidental coincidence background. Consequently, the error depends on the width of the coincidence window. For our data, minimum error is obtained for a window width of 12 to 14 channels ( $1.3\tau$ ). The quality factor, defined by Freedman,<sup>2</sup> was  $Q=1.03$  with the polarizers removed.

Figure 6 shows the polarization data for the full  $360^\circ$  together with a least-squares fit. The fitted parameters are in good agreement with the QM prediction, Eq. (5).

From the  $R_0$ ,  $R(22\frac{1}{2}^\circ)$ , and  $R(67\frac{1}{2}^\circ)$  data, we find

$$\delta_{\text{exp}} = 0.046 \pm 0.014 \quad (7)$$

in excellent agreement with the QM prediction, Eq. (6), and in clear violation of the LHV restriction, inequality (1).

The authors wish to thank the many people who have contributed to this work, especially Jim McGuire, Jim Ellis, Norman Alexander, and our instrument shop personnel.

\*Work supported by the Robert A. Welch Foundation, Grant No. A437, and by a grant from the Research Corporation.

<sup>1</sup>J. S. Bell, *Physics* (L. I. City, N. Y.) **1**, 195 (1965).

<sup>2</sup>S. J. Freedman, Lawrence Berkeley Laboratory Report No. LBL-391, 1972 (unpublished).

<sup>3</sup>J. F. Clauser and M. A. Horne, *Phys. Rev. D* **10**, 526 (1974).

<sup>4</sup>S. J. Freedman and J. F. Clauser, *Phys. Rev. Lett.* **28**, 938 (1972).

<sup>5</sup>R. A. Holt, Ph.D. thesis, Harvard University, 1973 (unpublished).

<sup>6</sup>J. F. Clauser, *Phys. Rev. Lett.* **36**, 1223 (1976).

<sup>7</sup>J. Blaise and H. Chantrel, *J. Phys. Radium* **18**, 193 (1957).

<sup>8</sup>E. S. Fry, *Phys. Rev. A* **8**, 1219 (1973).

## Stability of the Forward Multiplicity Ratios for $p$ - $p$ and $p$ -Aluminum Interactions at 28.5 GeV/c\*

L. J. Gutay, A. T. Laasanen, C. Ezell, and W. N. Schreiner†  
*Physics Department, Purdue University, West Lafayette, Indiana 47907*

and

F. Turkot

*Fermi National Accelerator Laboratory, Batavia, Illinois 60510*

(Received 5 April 1976)

We observe in the laboratory system that within a  $\theta = 20^\circ$  cone around the incident proton direction, the ratio of the average charged multiplicity for proton-aluminum interactions to that for proton-proton interactions is approximately 1 and is independent of missing mass and the transverse momentum of the trigger proton.

The conspicuous experimental results<sup>1</sup> for hadron collisions at very high energies prompted Gottfried to construct<sup>2,3</sup> the energy flux model (EFM). At 100- and 170-GeV/c incident pion momenta Busza *et al.*<sup>4</sup> have tested predictions of this model. In this Letter we study the apparent range of validity of the fundamental assumption on which EFM is based as a function of missing masses, momentum transfers, and incident energy.

To summarize the relevant experimental results and prediction of EFM, let  $\bar{n}_c^H$ ,  $\bar{n}_c^A$ , and  $R^A$  denote the average charged-particle multiplicities and their ratios ( $R^A = \bar{n}_c^A / \bar{n}_c^H$ ), respectively. The superscripts  $H$  and  $A$  denote that the average multiplicity in question was measured in  $p$ - $p$  or  $p$ -nucleus (nucleon number  $A$ ) interactions. The rather unexpected observation was that  $R^A$  at high energies is independent of incident beam momentum, and most important that  $R^A$  is small for all nuclei ( $1 \leq R^A < 2$ ). To explain this, one of EFM's assumptions (referred to later as "a") is that the interaction, between the incident proton and the array of nucleons in its path inside a nucleus, is completed in such a rapid succession that there is no time for the energy flux (EF), associated with the proton, to evolve from the proton state

into the predominant asymptotic states. Further the EF-nucleon interaction is dominated by elastic scattering. Assumption (a) leads to the conclusion (referred to later as "c") that if the incident energy is high enough to satisfy assumption (a), then the dependence of  $\bar{n}_c$  on the kinematic variables of  $p$ - $p$  and  $p$ -nucleus interactions are similar. Thus  $R^A$  in the hemisphere of the leading proton  $p_3$  is approximately one.

By carrying out our experiment at lower energies than Refs. 1 and 4, we show the following: (1) The interaction time of the  $p$ - $p$  interaction  $\tau_0$  is at least three times longer than estimated by Gottfried, and two times longer than what was measured by Busza *et al.*, thus extending the validity of assumption (a) to lower incident beam momenta. (2) By studying  $R^A$  as a function of the missing mass ( $M_3$ ) recoiling against  $p_3$ , we find that assumption (a) holds for inelasticities as large as  $\frac{3}{4}$ . (3) We show that assumption (a) holds when the fast forward proton emerges at large transverse momentum. (4) Energy deposition in the nucleus is dominated by meson production.

The experiment was carried out with the multi-particle ARGO spectrometer system (MASS). Using two spectrometers, namely the high-momen-